

## Structural and mechanistic insights into the inhibition of class C $\beta$ -lactamases through the adenylation of the nucleophilic serine

Min-Kyu Kim<sup>1,2†</sup>, Young Jun An<sup>1†</sup>, Jung-Hyun Na<sup>3†</sup>, Jae-Hee Seol<sup>1</sup>, Ju Yeon Ryu<sup>4</sup>, Jin-Won Lee<sup>5</sup>, Lin-Woo Kang<sup>6</sup>,  
Kyung Min Chung<sup>7</sup>, Jung-Hyun Lee<sup>1,8</sup>, Jeong Hee Moon<sup>4</sup>, Jong Seok Lee<sup>1,8</sup> and Sun-Shin Cha<sup>3\*†</sup>

<sup>1</sup>Marine Biotechnology Research Center, Korea Institute of Ocean Science and Technology (KIOST), Ansan, 15627, Republic of Korea; <sup>2</sup>Research Division for Biotechnology, Korea Atomic Energy Research Institute (KAERI), Jeongseup, 56212, Republic of Korea; <sup>3</sup>Department of Chemistry and Nano Science, Ewha Womans University, Seoul, 03760, Republic of Korea; <sup>4</sup>Functional Genomics Research Center, Korea Research Institute Bioscience and Biotechnology (KRIBB), Daejeon, 34141, Republic of Korea; <sup>5</sup>Department of Life Science, Hanyang University, Seoul, 04763, Republic of Korea; <sup>6</sup>Department of Biological Sciences, Konkuk University, Seoul, 05029, Republic of Korea; <sup>7</sup>Department of Microbiology and Immunology, Chonbuk National University Medical School, Jeonju, 54896, Republic of Korea; <sup>8</sup>Marine Biotechnology, Korea University of Science and Technology (UST), Daejeon, 34113, Republic of Korea

\*Corresponding author. Tel: +82-2-32774176; Fax: +82-2-32774546; E-mail: chajung@ewha.ac.kr

†These authors contributed equally to this work.

Received 7 June 2016; returned 9 August 2016; revised 5 October 2016; accepted 13 October 2016

**Objectives:** Investigation into the adenylation of the nucleophilic serine in AmpC BER and CMY-10 extended-spectrum class C  $\beta$ -lactamases.

**Methods:** The formation and the stability of the adenylylated adduct were examined by X-ray crystallography and MS. Inhibition assays for kinetic parameters were performed by monitoring the hydrolytic activity of AmpC BER and CMY-10 using nitrocefin as a reporter substrate. The effect of adenosine 5'-(P-acetyl)monophosphate (acAMP) on the MIC of ceftazidime was tested with four Gram-negative clinical isolates.

**Results:** The crystal structures and MS analyses confirmed the acAMP-mediated adenylylation of the nucleophilic serine in AmpC BER and CMY-10. acAMP inhibited AmpC BER and CMY-10 through the adenylylation of the nucleophilic serine, which could be modelled as a two-step mechanism. The initial non-covalent binding of acAMP to the active site is followed by the covalent attachment of its AMP moiety to the nucleophilic serine. The inhibition efficiencies ( $k_{\text{inact}}/K_{\text{I}}$ ) of acAMP against AmpC BER and CMY-10 were determined to be 320 and 140  $\text{M}^{-1} \text{s}^{-1}$ , respectively. The combination of ceftazidime and acAMP reduced the MIC of ceftazidime against the tested bacteria.

**Conclusions:** Our structural and kinetic studies revealed the detailed mechanism of adenylylation of the nucleophilic serine and may serve as a starting point for the design of novel class C  $\beta$ -lactamase inhibitors on the basis of the nucleotide scaffold.

### Introduction

$\beta$ -Lactam antibiotics are the most frequently prescribed antimicrobial agents.<sup>1</sup> However, their clinical application is challenged by the emergence and dissemination of bacterial resistance to these antibiotics. Expression of  $\beta$ -lactamases is a pervasive mechanism of resistance of bacteria to  $\beta$ -lactam antibiotics.  $\beta$ -Lactamases inactivate  $\beta$ -lactam antibiotics by opening the four-membered  $\beta$ -lactam ring that is essential for their efficacy. Efforts to evade  $\beta$ -lactamase-mediated inactivation led to the development of structurally diverse  $\beta$ -lactam antibiotics.<sup>2–4</sup> However, pathogens have evolved to express novel  $\beta$ -lactamases that are able to hydrolyse all kinds of  $\beta$ -lactam antibiotics.<sup>5,6</sup>

$\beta$ -Lactamases are divided into four classes, A, B, C and D, based on sequence homology.<sup>7</sup> Class C  $\beta$ -lactamases are widely

distributed among Gram-negative pathogens and are responsible for bacterial resistance to a broad spectrum of  $\beta$ -lactam antibiotics. Especially, extended-spectrum (ES) class C  $\beta$ -lactamases are capable of hydrolysing diverse  $\beta$ -lactam antibiotics, including cephamycins (cefoxitin and cefotetan), oxyimino cephalosporins (ceftazidime, cefotaxime and ceftiraxone), monobactams (aztreonam) and even imipenem.<sup>5,8,9</sup> The active site conformations of ES class C  $\beta$ -lactamases are modified by insertion, deletion or point mutations compared with those of their narrow-spectrum progenitors, and are directly related to their extended substrate range.<sup>6</sup> After the first identification of an ES class C  $\beta$ -lactamase in the *Enterobacter cloacae* clinical isolate GC1,<sup>10</sup> several chromosomal or

plasmidic ES class C  $\beta$ -lactamases have been reported in Enterobacteriaceae (*Klebsiella*, *Escherichia coli*, *Salmonella*) and the *Pseudomonas aeruginosa* TUH1529 isolate.<sup>5,9,11</sup>

The development of  $\beta$ -lactamase inhibitors is an effective strategy to cope with  $\beta$ -lactamase-mediated drug resistance. In fact, four  $\beta$ -lactamase inhibitors (clavulanate, sulbactam, tazobactam and avibactam) are clinically used in combination with  $\beta$ -lactam antibiotics (e.g. amoxicillin/clavulanate, ticarcillin/clavulanate, ampicillin/sulbactam, piperacillin/tazobactam, cefoperazone/sulbactam and ceftazidime/avibactam). These clinical inhibitors are especially active against class A enzymes, displaying much less or no effect on other classes of  $\beta$ -lactamases except for avibactam, which also inhibits class C and some class D  $\beta$ -lactamases.<sup>3,12–16</sup> In addition,  $\beta$ -lactamases resistant to the existing inhibitors are emerging,<sup>17</sup> highlighting the need to develop novel inhibitors. In this article, we describe the structure-guided discovery of the adenylation-mediated inhibition of class C  $\beta$ -lactamases, and present structural and kinetic analyses of this inhibition mode.

## Materials and methods

### Enzyme preparation and crystal structure determination

Detailed procedures for cloning, expression, purification, crystallization, data collection and crystal structure determinations are described in Supplementary Materials and methods (available as Supplementary data at JAC online).

### Purification of $\beta$ -lactamases by *m*-aminophenylboronic acid (mAPBA) resin

Adenylylated and unadenylylated forms of AmpC BER and CMY-10 were separated by using mAPBA resin (Sigma, USA; Table S1). Briefly, purified AmpC BER (20 mg) or CMY-10 (20 mg) was mixed with mAPBA resin (2 mL). The unadenylylated enzymes with intact nucleophilic serines bound to the resin and were eluted using a buffer containing 500 mM sodium borate, pH 7.0, and 500 mM sodium chloride, whereas the adenylylated enzymes passed through the resin. After the final purification step with mAPBA resin, intact nucleophilic serines of unadenylylated AmpC BER and CMY-10 were confirmed by MS analyses (Table S1, available as Supplementary data at JAC Online). Adenylylated and unadenylylated enzymes were also verified by monitoring time-dependent nitrocefirin hydrolysis at 486 nm ( $\epsilon = 20\,500\text{ M}^{-1}\text{ cm}^{-1}$ ) using a SpectraMAX Plus spectrophotometer (Molecular Devices, USA; Figure S1). Except for NDM-1 (a class B enzyme with no nucleophilic serine), all  $\beta$ -lactamases used in this study were purified by using mAPBA resin to clarify their intact nucleophilic serines.

### Stability of adenylylated nucleophilic serine and reactivation assays

Unadenylylated AmpC BER (4  $\mu\text{M}$ ) and CMY-10 (4  $\mu\text{M}$ ) were incubated with 500  $\mu\text{M}$  5'-(*P*-acetyl)monophosphate (acAMP) in a buffer of 20 mM MES, pH 6.5, for 2 h at room temperature. Excess acAMP was removed by ultrafiltration and subsequent washing steps. To examine the stability of the adenylylated nucleophilic serine, the resultants were incubated for 5 days at room temperature and then subject to MS analyses.

The reactivation of inactivated AmpC BER and CMY-10 was monitored using a jump dilution method.<sup>18</sup> Unadenylylated AmpC BER (8  $\mu\text{M}$ ) and CMY-10 (4  $\mu\text{M}$ ) were completely inactivated by 200  $\mu\text{M}$  avibactam, 500  $\mu\text{M}$  acAMP or 5 mM clavulanate for 2 h at room temperature. To remove excess inhibitors, the inactivated enzymes were immediately diluted 8000-fold in a buffer (50 mM MES, pH 6.5) with or without inhibitors. The reactivation of the enzyme activity was measured in a solution containing 100  $\mu\text{M}$  nitrocefirin for 16 h (CMY-10) or 18 h (AmpC BER).

### Inhibition assays

To test the inhibitory effect of AMP-containing compounds (Figure S2) against  $\beta$ -lactamases, AmpC BER (0.4 nM), AmpC EC2 (0.2 nM), CMY-10 (0.2 nM), CMY-2 (0.2 nM), NDM-1 (0.4 nM), KPC-2 (0.2 nM), TEM-1 (0.5 nM), OXA-10 (0.2 nM) and OXA-48 (0.2 nM) were preincubated with each compound (2 mM) in a 50 mM MES, pH 6.5, buffer at room temperature for 5 min. Then, enzyme activity was measured after the addition of 100  $\mu\text{M}$  nitrocefirin at 486 nm for 1 h. The measured enzyme activities were quantified based on a percentage according to the following equation:  $(v_i/v_0 \times 100)$ , where  $v_i$  and  $v_0$  are the initial velocity in the presence and absence of AMP-containing compounds, respectively.

To determine kinetic constants of acAMP, avibactam and clavulanate, the hydrolysis of nitrocefirin by AmpC BER (0.4 nM) or CMY-10 (0.2 nM) was continuously observed in the presence of 20–400  $\mu\text{M}$  acAMP, 0.5–25  $\mu\text{M}$  avibactam or 500–3500  $\mu\text{M}$  clavulanate. Their inhibition modes were fitted to a two-step model (Equation 1):<sup>16,19</sup>



In the case of acAMP,  $k_{-2}$  is zero because there was no dissociation of the covalent E-I complex (see the Inhibition kinetics of acAMP section in the Results and discussion section).<sup>20</sup>

Time courses were fitted to Equation 2 to obtain the pseudo-first-order rate constant,  $k_{\text{obs}}$ .<sup>16,19,21</sup>

$$[P] = v_s t + (v_0 - v_s) \frac{(1 - e^{-k_{\text{obs}} t})}{k_{\text{obs}}} \quad (2)$$

where [P] is the concentration of the product,  $v_0$  and  $v_s$  represent the initial and final reaction velocity, respectively, and  $t$  is time.<sup>19,21</sup> When a saturation curve was obtained from the  $k_{\text{obs}}$  versus [I] graph,  $k_{\text{obs}}$  was fitted to Equation 3 to obtain the values of  $k_{\text{inact}}$  and  $K_1$  that represent the maximum rate of inactivation and the inhibitor concentration that yields half the maximum rate of inactivation ( $1/2 k_{\text{inact}}$ ), respectively.<sup>20,22</sup>

$$k_{\text{obs}} = k_{-2} + k_{\text{inact}} \frac{[I]}{K_1 \left(1 + \frac{[S]}{K_m}\right) + [I]} \quad (3)$$

When the plot of  $k_{\text{obs}}$  versus [I] was linear,  $k_{\text{obs}}$  was fitted to Equation 4 to obtain the value of  $k_2/K$ <sup>21,22</sup> that corresponds to the slope of the graph, where  $K = k_{-1}/k_1$ .<sup>16</sup>

$$k_{\text{obs}} = k_{-2} + \frac{k_2}{K} \frac{[I]}{\left(1 + \frac{[S]}{K_m}\right)} \quad (4)$$

$k_{\text{inact}}/K_1$  and  $k_2/K$  are the second-order rate constants that are generally used for comparing inhibitor efficiencies.<sup>22</sup> The reported value for the  $k_{\text{obs}}$  versus [I] slope includes an adjustment for the  $(1 + [S]/K_m)$  term to account for the nitrocefirin substrate concentration ( $[S] = 100\text{ }\mu\text{M}$ ,  $K_m$  of 34.9  $\mu\text{M}$  for AmpC BER and 20.8  $\mu\text{M}$  for CMY-10).<sup>19,22,23</sup> The reported values were calculated using Origin software (OriginLab, USA).

### Antimicrobial susceptibility testing

The MIC values were determined by using the broth microdilution method with an inoculum of  $5 \times 10^5$  cfu/mL according to CLSI guidelines.<sup>24,25</sup> Avibactam, acAMP and clavulanate were tested for synergy with the third-generation  $\beta$ -lactam ceftazidime against a clinically isolated *E. coli*

producing AmpC BER<sup>11</sup> and three ceftazidime-resistant clinical isolates (*Enterobacter aerogenes*, *Klebsiella pneumoniae* and *Acinetobacter baumannii*). The MIC value of ceftazidime in combination with avibactam had been determined with the recombinant *E. coli* TOP10 strain transformed by a plasmid encoding the *ampC BER* gene.<sup>26</sup> The lowest concentration of ceftazidime that prevented visible bacterial growth after overnight incubation at 37 °C was taken as the MIC.

## Results and discussion

### Adenylylated serine in the active site of AmpC BER

AmpC BER from an *E. coli* clinical isolate is an ES class C enzyme with a two-residue insertion in the H10 helix (residues 289–296) compared with its progenitor AmpC EC2.<sup>9</sup> According to the crystal structure (Table S2), it adopts a two-domain structure with the active site at the domain interface (Figure 1a), similar to other class C  $\beta$ -lactamases. Hereafter, residues are numbered according to the canonical numbering of *E. cloacae* P99 AmpC.<sup>27</sup> An  $\alpha/\beta$  domain (residues 5–81 and 169–363) has a central sheet sandwiched by helices and an  $\alpha$ -helical domain (residues 82–168) is exclusively composed of helices.

Class C enzymes have a nucleophilic serine that attacks the carbonyl carbon of the  $\beta$ -lactam ring to open the ring. From the initial stage of refinement, we observed a well-defined electron density directly connected to the nucleophilic serine (Ser-64) (Figure 1b and c). Since we added no substrates or inhibitors during purification and crystallization, the observation of an adduct was unexpected. Interpretation of the 1.76 Å resolution electron-density maps revealed that the nucleophilic Ser-64 is adenylylated. The hydroxyl oxygen of Ser-64 is covalently linked to the phosphorus atom of AMP (Figure 1b and c). This is further supported by electrospray ionization–tandem MS (ESI–MS/MS). The tryptic peptides containing Ser-64 (<sup>51</sup>KQPVTQQLFELGVSVK<sup>67</sup>) were detected as

two peaks: one with the expected  $m/z$  value (60.9%,  $m/z = 945.4$  and 630.7 for doubly and triply charged ions, respectively) and the other with a 329 Da mass shift corresponding to the mass of phosphoadenosine (39.1%,  $m/z = 1110.0$  and 740.4 for doubly and triply charged ions, respectively) (Figure S3 and Table S1). MS/MS analysis of the peptide with a 329 Da mass shift ( $m/z = 1110.0$ ) (Figure S3), together with crystallographic observation (Figure 1b and c), showed that Ser-64 is the adenylylation site. Since we had not been aware of the existence of two mass isoforms of recombinant AmpC BER, we had used the mixture for crystallization. Therefore, it appears that only adenylylated AmpC BER was crystallized in our crystallization condition. Consistently, occupancy refinement revealed that the occupancy of the AMP adduct is 1.00.

We obtained AmpC BER from cells cultured in M9 minimal media and also observed the adenylylated Ser-64 in this preparation (Table S1), indicating that the AMP adduct did not originate from the LB medium that was originally used to obtain recombinant AmpC BER. It is notable that adenylylation of nucleophilic serine was also reported in the cytoplasmically expressed class C  $\beta$ -lactamase FOX-4.<sup>28</sup> In the case of periplasmically expressed FOX-4, however, no adenylylation was observed, suggesting that the source of the AMP adduct is an AMP-containing metabolite in the cytoplasm. Considering that  $\beta$ -lactamases are periplasmic proteins, the intentional deletion of signal peptides of AmpC BER and FOX-4 to locate them in the cytoplasm is highly likely to be responsible for their biologically irrelevant encounter with cytoplasmic AMP-containing metabolites. Consequently, the adenylylation of  $\beta$ -lactamases is not likely to occur in the native host and thus the observed adenylylation of AmpC BER and FOX-4 is probably artefactual rather than having biological implications. Hereafter, AmpC BER adenylylated in the cytoplasm is referred to as AmpC BER-CA to discriminate it from AmpC BER adenylylated by acAMP (see below).

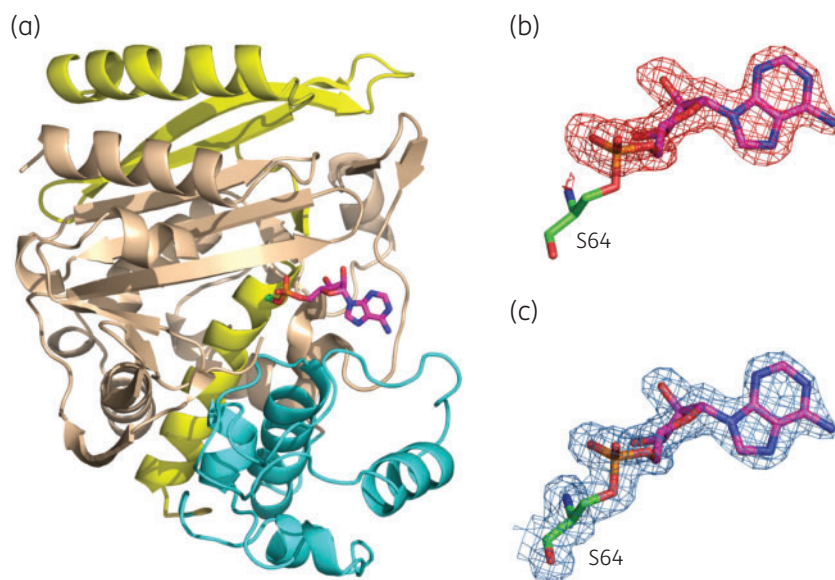


**Figure 1.** Crystal structure of adenylylated AmpC BER-CA. (a) An  $\alpha/\beta$  domain (residues 5–81 in yellow and 169–363 in wheat) and an  $\alpha$ -helical domain (residues 82–168 in cyan) are shown as a cartoon. Ser-64 (green) and covalently bound AMP (magenta) are shown as sticks. Nitrogen, oxygen and phosphorus atoms are coloured blue, red and orange, respectively. Initial maximum-likelihood-weighted (b)  $F_o - F_c$  and (c)  $2F_o - F_c$  electron-density maps contoured at  $1\sigma$  and  $3\sigma$ , respectively, for adenylylated Ser-64 in the final model.

### Dissection of the AMP binding mode

The phosphorus atom of AMP is surrounded by four oxygen atoms, including the hydroxyl oxygen of Ser-64 in a tetrahedral arrangement (Figure S4). 5'-Hydroxyl oxygen is hydrogen-bonded to Lys-67 and one terminal oxygen atom (O1) makes hydrogen bonds with the backbone -NH groups of Ser-64 and Ala-320 (Figure S4). The other terminal oxygen atom (O3) directly interacts with the hydroxyl group of Tyr-150 and forms water-mediated interactions with Asn-348 and Arg-351 (Figure S4). Similar tetrahedral arrangements around the phosphorus atom were also observed in covalent adducts formed between phosphonate inhibitors and the nucleophilic serine of  $\beta$ -lactamases.<sup>29-35</sup> The tetrahedral geometry with one oxygen atom at the oxyanion hole resembles the tetrahedral intermediate of the acylation part of the  $\beta$ -lactamase-catalysed reaction.

The ribose ring is packed against the aromatic ring of Tyr-221 with its 3'-OH hydrogen bonding with the backbone -CO group of Ala-320 (Figure S4). The 2'-OH of the ribose makes a hydrogen bond with a

nearby sulphate ion that is a component of the mother liquor for crystallization: the sulphate ion directly interacts with the backbone -NH groups of Ser-212 and Gly-322, and forms water-mediated interactions with the side chain of Glu-61 and the backbone -CO group of His-210 (Figure S4). The ribose ring oxygen (O4') is 4 Å away from the side-chain amide nitrogen atom of Asn-152 (Figure S4). The pyrimidine ring and the imidazole ring in the adenine moiety make van der Waals contact with the side chains of Gln-120 and Tyr-221, respectively (Figure S4). NH<sub>2</sub> at C-6 interacts with the side-chain carboxylate oxygens of Asp-123 and Gln-120 and the backbone -CO group of Val-121. N7 forms a water-mediated interaction with the backbone -NH group of Val-121 (Figure S4).

### Inhibitory activities of AMP-containing metabolites

The accommodation of AMP in the active site led us to test whether AMP-containing compounds (Figure S2) inhibit ES class C

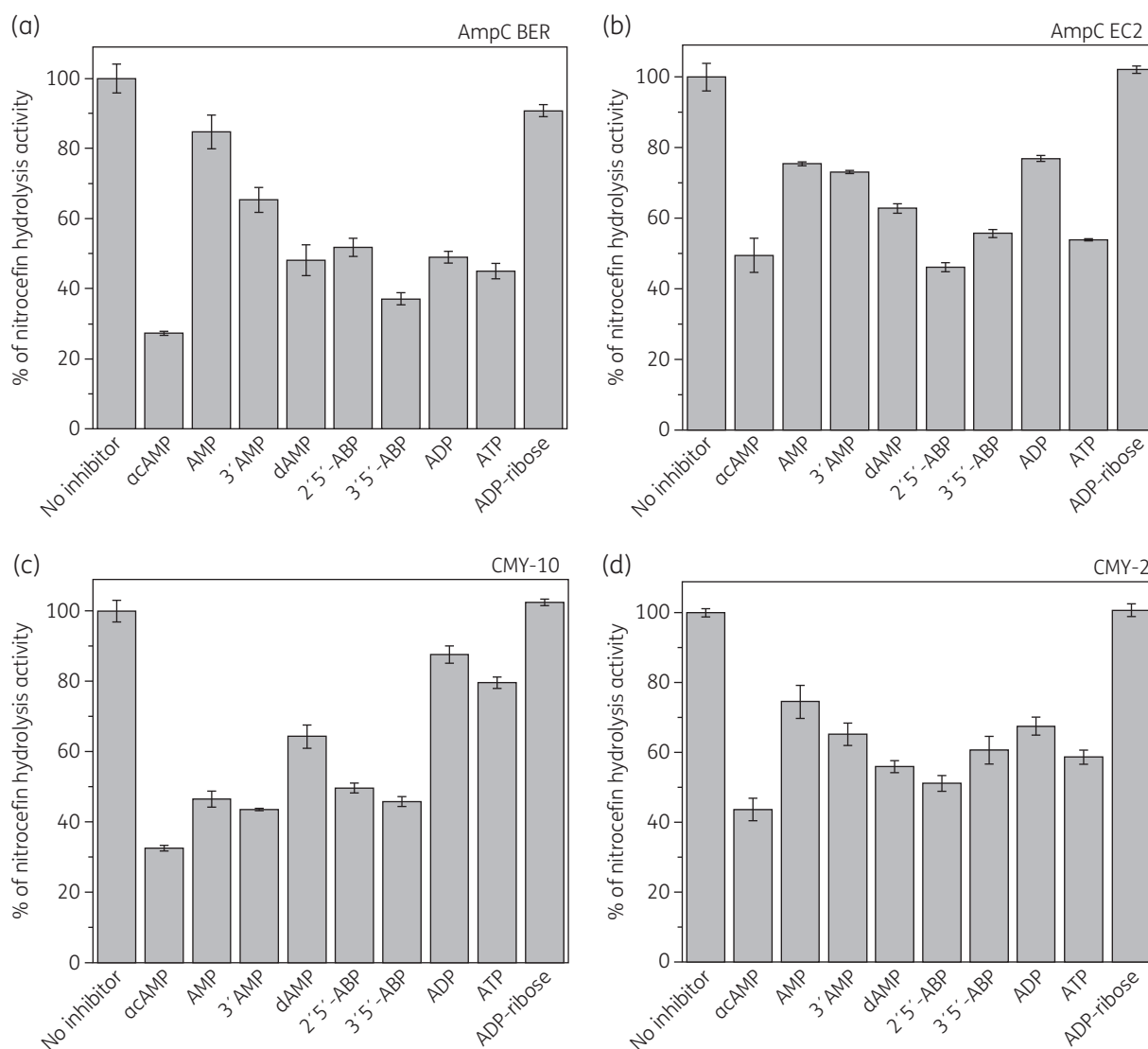


**Figure 2.** Inhibitory effects of AMP-containing compounds against class C  $\beta$ -lactamases. Percentage changes in the nitrocefin-hydrolysing activity of (a) Amp BER, (b) AmpC EC2, (c) CMY-10 and (d) CMY-2 in the presence of AMP-containing metabolites. Error bars are  $\pm$  SD for triplicate experiments.

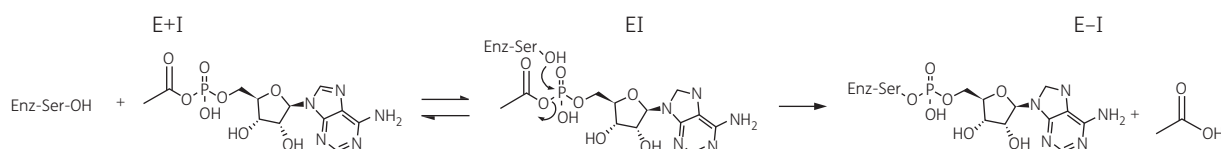


**Figure 3.** Proposed steps of adenylation of nucleophilic serine. Enz-Ser-OH represents the nucleophilic serine.

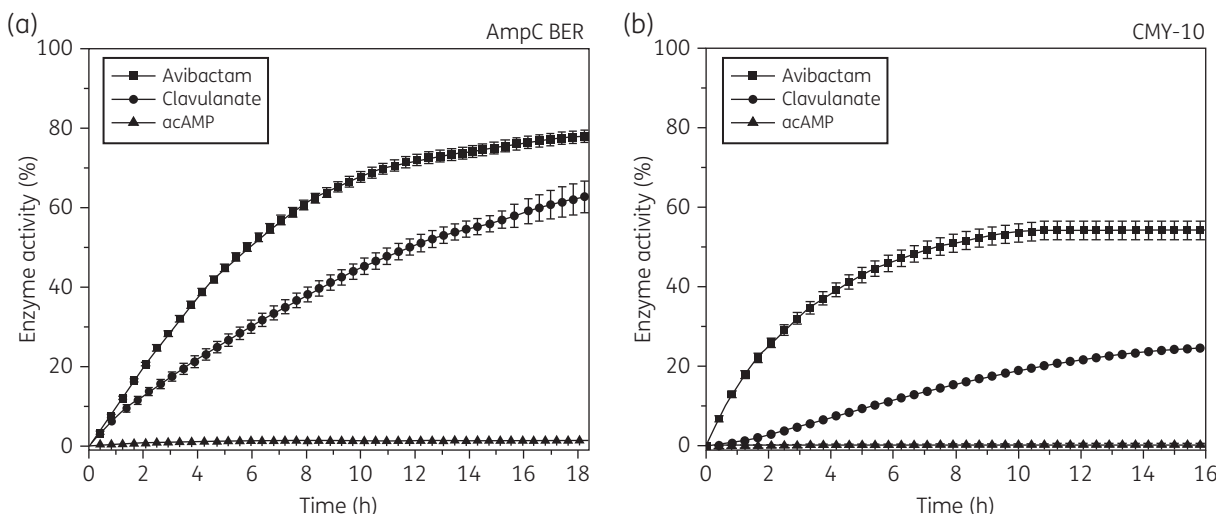


**Figure 4.** Time courses of AmpC BER and CMY-10 reactivation. After complete inactivation of (a) AmpC BER and (b) CMY-10 by 500  $\mu$ M acAMP (triangles), 50  $\mu$ M avibactam (squares) or 1 mM clavulanate (circles), their nitrocefins-hydrolysing activities were monitored for 18 h (AmpC BER) and 16 h (CMY-10), respectively. Error bars are  $\pm$ SD for triplicate experiments.

enzymes (AmpC BER and CMY-10) and their progenitors (AmpC EC2 and CMY-2).<sup>11</sup> Interestingly, most compounds reduced nitrocefins hydrolysis by >20%, which showed the inhibition efficacy of the AMP moiety towards class C enzymes (Figure 2). Additionally, to test the inhibition spectrum of these compounds, we performed the same inhibition experiments with class A (KPC-2 and TEM-1), class B (NDM-1) and class D (OXA-10 and OXA-48) enzymes. Some compounds were effective on KPC-2, only acAMP showed weak inhibition activities against OXA-10 and OXA-48, but all tested compounds failed to exhibit clear inhibition activities against TEM-1 and NDM-1 (Figure S5). Overall, the tested AMP-containing compounds were more effective on class C enzymes than other classes.

### Adenylation of nucleophilic serine in AmpC BER and CMY-10 by acAMP

acAMP is a cytosolic metabolite<sup>36</sup> composed of adenosine-phosphate-acetyl (Figure 3). If the nucleophilic serine attacked the phosphorus atom of the phospho-carboxylic anhydride bond between phosphate and acetyl, the AMP moiety of acAMP would be transferred to the nucleophilic serine, releasing acetyl (Figure 3). Taken together, acAMP, which can be synthesized through a simple reaction (Figure S6),<sup>37</sup> was an ideal molecule to demonstrate the covalent attachment of AMP to the serine, as observed in the crystal structure of AmpC BER-CA.

Although KPC-2, OXA-10 and OXA-48 were slightly inhibited by acAMP, class C  $\beta$ -lactamases, particularly ES class C  $\beta$ -lactamases, were significantly inhibited by acAMP. As a first step towards

verifying acAMP-mediated adenylation, therefore, we determined the structures of unadenylated AmpC BER and CMY-10 (Tables S1 and S2) with crystals grown in the presence of acAMP (Table S2), and observed the anticipated AMP adduct covalently linked to the nucleophilic serine (Figures S7 and S8). The binding modes of the AMP adducts in these structures are virtually identical to that in the crystal structure of AmpC BER-CA (Figures S4 and S9). This result supports our assumption that the source of the AMP adduct observed in the crystal structure of AmpC BER-CA (Figure 1) is an AMP-containing metabolite in the cytoplasm, although we cannot specify acAMP as the metabolite responsible for the observed adenylation at this stage.

### Inhibition kinetics of acAMP

According to the stability test, the adenylylated serines of AmpC BER and CMY-10 were maintained for 5 days (Table S1). Consistently, AmpC BER and CMY-10 completely inhibited by acAMP displayed no reactivation during 18 and 16 h, respectively (Figure 4), indicating the stable nature of the adenylate adduct. In contrast, the reactivation of AmpC BER and CMY-10 inhibited by avibactam was observed to follow a time-dependent course (Figure 4), which is compatible with a previous study that avibactam is a covalent and reversible inhibitor.<sup>19</sup> The enzymes inhibited by clavulanate were also recovered in a time-dependent manner (Figure 4).

After demonstrating that acAMP is a covalent irreversible inhibitor, we determined the observed first-order rate constant ( $k_{\text{obs}}$ ) of AmpC BER and CMY-10 (Figure 5). Plots of  $k_{\text{obs}}$  as a function of [acAMP] are non-linear (Figure 5), which is compatible

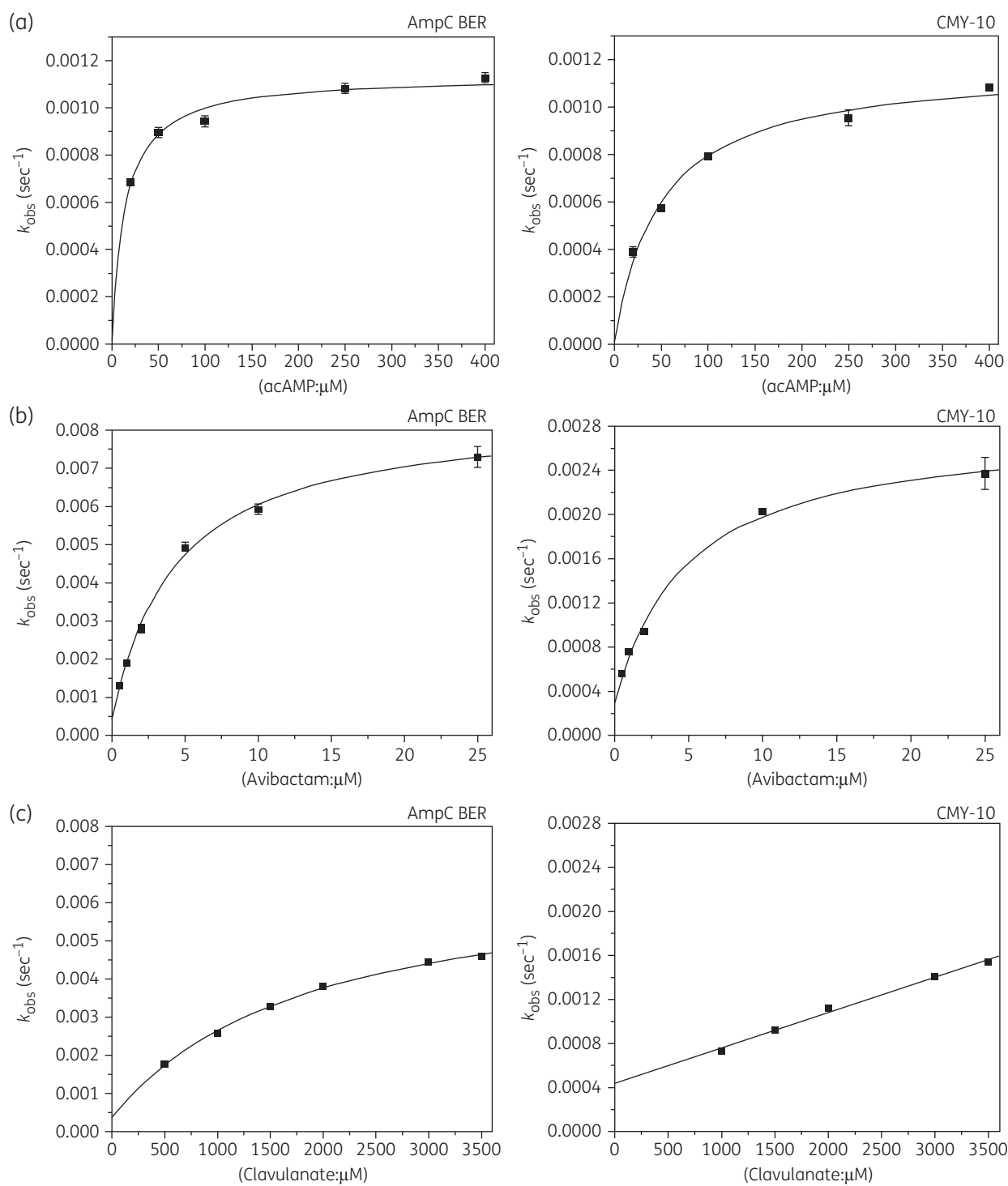


**Figure 5.** Plots of  $k_{\text{obs}}$  versus (a) [acAMP], (b) [avibactam] or (c) [clavulanate] for AmpC BER and CMY-10. Plots were fitted as described in the Materials and methods section to obtain the second-order rate constants ( $k_{\text{inact}}/K_1$  or  $k_2/K$ ). Error bars are  $\pm$ SD for triplicate experiments.

**Table 1.** Kinetic values for the inhibitory activities of acAMP, avibactam and clavulanate against AmpC BER and CMY-10

Inhibitor/enzyme	$k_{\text{inact}}$ ( $\text{s}^{-1}$ )	$K_{\text{I}}$ ( $\mu\text{M}$ )	$k_{\text{inact}}/K_{\text{I}}$ ( $\text{M}^{-1}\text{s}^{-1}$ )
acAMP			
AmpC BER	$1.1 \times 10^{-3} \pm 3 \times 10^{-5}$	$3.6 \pm 0.6$	$3.2 \times 10^2 \pm 4$
CMY-10	$1.2 \times 10^{-3} \pm 8 \times 10^{-5}$	$8.2 \pm 2$	$1.4 \times 10^2 \pm 5$
Avibactam			
AmpC BER	$8.1 \times 10^{-3} \pm 3 \times 10^{-4}$	$1.1 \pm 0.2$	$7.2 \times 10^3 \pm 9 \times 10^2$
CMY-10	$2.5 \times 10^{-3} \pm 8 \times 10^{-5}$	$0.83 \pm 0.2$	$3.0 \times 10^3 \pm 4 \times 10^2$
Clavulanate			
AmpC BER	$6.6 \times 10^{-3} \pm 3 \times 10^{-4}$	$4.8 \times 10^2 \pm 1 \times 10^2$	$14 \pm 0.1$
Inhibitor/enzyme	$k_2$ ( $\text{s}^{-1}$ )	$K$ ( $\mu\text{M}$ )	$k_2/K$ ( $\text{M}^{-1}\text{s}^{-1}$ )
Clavulanate			
CMY-10	ND	ND	$1.9 \pm 0.07$

ND, not determined.

Values are means  $\pm$  SD for triplicate experiments.

**Table 2.** MIC values of ceftazidime alone and in combination with acAMP, avibactam and clavulanate for clinically isolated bacteria

Compound	MIC (mg/L)			
	<i>E. coli</i> BER producing AmpC BER	<i>E. aerogenes</i> <sup>a</sup>	<i>K. pneumoniae</i> <sup>b</sup>	<i>A. baumannii</i> <sup>c</sup>
Ceftazidime	128	32	128	> 512
+ 1 mM acAMP	128	32	128	> 512
+ 2 mM acAMP	64	32	128	> 512
+ 2.5 mM acAMP	32	16	128	512
+ 5 mM acAMP	< 32	2	64	32
+ 0.02 mM AVI	128	16	128	512
+ 0.05 mM AVI	128	1	16	16
+ 0.1 mM AVI	128	< 1	< 16	< 16
+ 0.2 mM AVI	64	< 1	< 16	< 16
+ 0.25 mM AVI	< 32	< 1	< 16	< 16
+ 2.5 mM CLA	128	NT	NT	NT

NT, not tested; AVI, avibactam; CLA, clavulanate.

Organisms other than *E. coli* BER were purchased from Culture Collection of Antimicrobial Resistance Microbes (CCARM, Republic of Korea).

<sup>a</sup>CCARM 16006.

<sup>b</sup>CCARM 10255.

<sup>c</sup>CCARM 12001.

with a two-step inhibition mechanism (Equation 1).<sup>22</sup> The first step corresponds to the reversible non-covalent binding of acAMP to the active site. The second step involves irreversible adenylation of the nucleophilic serine.<sup>22</sup> The inhibition efficiency ( $k_{\text{inact}}/K_{\text{I}}$ ) was obtained from the plots. The inhibition efficiencies of acAMP against AmpC BER and CMY-10 (Figure 5) were  $\sim$ 20-fold lower than those of avibactam (Table 1 and Figure 5).<sup>17,19</sup> Interestingly, inhibition efficiencies of acAMP towards AmpC BER and CMY-10 were  $\sim$ 20 and  $\sim$ 70-fold higher than those of clavulanate (Table 1 and Figure 5), respectively. It is notable that non-linear plots of  $k_{\text{obs}}$  versus [avibactam] presented in this study show the saturating inhibition of AmpC BER and CMY-10 by avibactam, since so far the plots of  $k_{\text{obs}}$  versus [avibactam] for other  $\beta$ -lactamases were typically linear even at high avibactam concentrations.<sup>16,19,21</sup>

### Influence of acAMP on the MIC of ceftazidime

To investigate the influence of acAMP on the MIC of ceftazidime against bacteria expressing class C  $\beta$ -lactamases (Table 2), we chose a ceftazidime-resistant *E. coli* clinical isolate producing AmpC BER<sup>11</sup> as a model cell. Although acAMP has no effect on MIC at low concentrations, 2 mM acAMP reduced the MIC values of ceftazidime by 50% (Table 2). acAMP alone did not prevent bacterial growth at all even at 5 mM concentration, indicating that the metabolite has no cytotoxic activity. The MIC value of ceftazidime against the *E. coli* BER strain was reduced to 50% in the presence of 0.2 mM avibactam, whereas clavulanate had no effect on the MIC values even at 2.5 mM (Table 2). The effective concentration of acAMP for reducing the MIC is  $\sim$ 10 fold higher than that of avibactam, which is compatible with the observation that the inhibition efficiency ( $k_{\text{inact}}/K_{\text{I}}$ ) of acAMP towards AmpC BER is  $\sim$ 20-fold

lower than that of avibactam (Table 1). Comparing  $K_I$  and  $k_{inact}$  values of acAMP and avibactam (Table 1), the different inhibition efficiencies of the two inhibitors seem to be more related to the disparity in the  $k_{inact}$  values. Therefore, the effectiveness of acAMP would be substantially enhanced if its structure were appropriately modified to improve covalent bond formation.

We also performed antimicrobial susceptibility testing with clinically isolated Gram-negative bacteria (*E. aerogenes*, *K. pneumoniae* and *A. baumannii*), whose genes conferring  $\beta$ -lactam resistance have not yet been identified. acAMP at 2.5–5 mM reduced the MIC values of ceftazidime by  $\sim 2$ –16-fold against the three clinical isolates (Table 2), while avibactam was effective in reducing the MIC value by  $\sim 10$ -fold at much lower concentrations (0.05 mM). Without information on the class of  $\beta$ -lactamases expressed in the three clinical isolates, it is difficult to elucidate the reason for the large disparity in effective concentration between class C-specific acAMP and avibactam, displaying a broad spectrum of effectiveness against class A, C and some D enzymes.<sup>16</sup>

In conclusion, we discovered that class C  $\beta$ -lactamases accommodate AMP, a basic building block of RNA, and demonstrated that the adenylation of the nucleophilic serine is effective in inhibiting the enzymes. Our findings suggest that acAMP is a lead compound for the development of non- $\beta$ -lactam irreversible covalent inhibitors. The attachment of the adenosine moiety to the  $\beta$ -lactam ring or the diazabicyclooctane might also be applied to design new  $\beta$ -lactamase inhibitors. Atomic details of the interactions of AMP with the active sites of AmpC BER and CMY-10 will be invaluable for the structure-based optimization of the nucleotide scaffold, a natural chemical space that has been successfully exploited to develop drugs for cancer and viral diseases<sup>38</sup> but has never been explored in searching for  $\beta$ -lactamase inhibitors.

## Acknowledgements

We thank Professor Patrice Nordmann for providing the *E. coli* BER strain, Professor Sahriar Mobashery for providing the OXA-10 clone, and the beamline staffs at PLS and PF for support with the data collection. Avibactam was a kind gift from LegoChem Bio, Republic of Korea.

## Funding

This study was supported by National Research Foundation of Korea grants (NRF-2015R1A2A2A01004168 and NRF-2015M1A5A1037480), the KIOST in-house programs (PE99413 and PE99302) and a grant from the Marine Biotechnology Program (PJT200620) funded by the Ministry of Oceans and Fisheries, Korea. Mass spectrometry experiments were supported by a grant from the KRIBB Research Initiative Program.

## Transparency declarations

None to declare.

## Supplementary data

Supplementary Materials and methods, Figures S1 to S9, and Tables S1 and S2, available as Supplementary data at JAC Online are available as Supplementary data at JAC Online (<http://jac.oxfordjournals.org/>).

## References

- Liu XL, Shi Y, Kang JS et al. Amino acid thioester derivatives: a highly promising scaffold for the development of metallo- $\beta$ -lactamase L1 inhibitors. *ACS Med Chem Lett* 2015; **6**: 660–4.
- Dalhoff A, Janjic N, Echols R. Redefining penems. *Biochem Pharmacol* 2006; **71**: 1085–95.
- Drawz SM, Bonomo RA. Three decades of  $\beta$ -lactamase inhibitors. *Clin Microbiol Rev* 2010; **23**: 160–201.
- Miller AK, Celozzi E, Kong Y et al. Cephamycins, a new family of  $\beta$ -lactam antibiotics. IV. *In vivo* studies. *Antimicrob Agents Chemother* 1972; **2**: 287–90.
- Bradford PA. Extended-spectrum  $\beta$ -lactamases in the 21st century: characterization, epidemiology, and detection of this important resistance threat. *Clin Microbiol Rev* 2001; **14**: 933–51.
- Paterson DL, Bonomo RA. Extended-spectrum  $\beta$ -lactamases: a clinical update. *Clin Microbiol Rev* 2005; **18**: 657–86.
- Hall BG, Barlow M. Revised Ambler classification of  $\beta$ -lactamases. *J Antimicrob Chemother* 2005; **55**: 1050–1.
- Rodríguez-Martínez JM, Poirel L, Nordmann P. Extended-spectrum cephalosporinases in *Pseudomonas aeruginosa*. *Antimicrob Agents Chemother* 2009; **53**: 1766–71.
- Nordmann P, Mammeri H. Extended-spectrum cephalosporinases: structure, detection and epidemiology. *Future Microbiol* 2007; **2**: 297–307.
- Crichlow GV, Kuzin AP, Nukaga M et al. Structure of the extended-spectrum class C  $\beta$ -lactamase of *Enterobacter cloacae* GC1, a natural mutant with a tandem tripeptide insertion. *Biochemistry* 1999; **38**: 10256–61.
- Mammeri H, Poirel L, Nordmann P. Extension of the hydrolysis spectrum of AmpC  $\beta$ -lactamase of *Escherichia coli* due to amino acid insertion in the H-10 helix. *J Antimicrob Chemother* 2007; **60**: 490–4.
- Bush K.  $\beta$ -Lactamase inhibitors from laboratory to clinic. *Clin Microbiol Rev* 1988; **1**: 109–23.
- Buynak JD. Understanding the longevity of the  $\beta$ -lactam antibiotics and of antibiotic/ $\beta$ -lactamase inhibitor combinations. *Biochem Pharmacol* 2006; **71**: 930–40.
- Cantón R, Coque TM. The CTX-M  $\beta$ -lactamase pandemic. *Curr Opin Microbiol* 2006; **9**: 466–75.
- Philippon A, Labia R, Jacoby G. Extended-spectrum  $\beta$ -lactamases. *Antimicrob Agents Chemother* 1989; **33**: 1131–6.
- Ehmann DE, Jahić H, Ross PL et al. Kinetics of avibactam inhibition against class A, C, and D  $\beta$ -lactamases. *J Biol Chem* 2013; **288**: 27960–71.
- Garber K. A  $\beta$ -lactamase inhibitor revival provides new hope for old antibiotics. *Nat Rev Drug Discov* 2015; **14**: 445–7.
- Copeland RA, Basavapathruni A, Moyer M et al. Impact of enzyme concentration and residence time on apparent activity recovery in jump dilution analysis. *Anal Biochem* 2011; **416**: 206–10.
- Ehmann DE, Jahić H, Ross PL et al. Avibactam is a covalent, reversible, non- $\beta$ -lactam  $\beta$ -lactamase inhibitor. *Proc Natl Acad Sci USA* 2012; **109**: 11663–8.
- Singh J, Pettec RC, Baillie TA et al. The resurgence of covalent drugs. *Nat Rev Drug Discov* 2011; **10**: 307–17.
- Xu H, Hazra S, Blanchard JS. NXL104 irreversibly inhibits the  $\beta$ -lactamase from *Mycobacterium tuberculosis*. *Biochemistry* 2012; **51**: 4551–7.
- Copeland RA. *Evaluation of Enzyme Inhibitors in Drug Discovery: A Guide for Medicinal Chemists and Pharmacologists*. Hoboken, NJ: Wiley-Interscience, 2005.
- Stachyra T, Pêcheureau MC, Bruneau JM et al. Mechanistic studies of the inactivation of TEM-1 and P99 by NXL104, a novel non- $\beta$ -lactam  $\beta$ -lactamase inhibitor. *Antimicrob Agents Chemother* 2010; **54**: 5132–8.
- Clinical and Laboratory Standards Institute. *Performance Standards for Antimicrobial Susceptibility Testing*. M100-S25. Wayne, PA, USA, 2015.



- 25** Clinical and Laboratory Standards Institute. *Methods for Dilution Antimicrobial Susceptibility Tests for Bacteria That Grow Aerobically; Approved Standard*. M07-A10. Wayne, PA, USA, 2015.
- 26** Pores-Osante N, Dupont H, Torres C *et al*. Avibactam activity against extended-spectrum AmpC  $\beta$ -lactamases. *J Antimicrob Chemother* 2014; **69**: 1715–6.
- 27** Galleni M, Lindberg F, Normark S *et al*. Sequence and comparative analysis of three *Enterobacter cloacae ampC*  $\beta$ -lactamase genes and their products. *Biochem J* 1988; **250**: 753–60.
- 28** Lefurgy ST, Malashkevich VN, Aguilan JT *et al*. Analysis of the structure and function of FOX-4 cephamycinase. *Antimicrob Agents Chemother* 2016; **60**: 717–28.
- 29** Curley K, Pratt RF. Effectiveness of tetrahedral adducts as transition-state analogs and inhibitors of the class C  $\beta$ -lactamase of *Enterobacter cloacae* P99. *J Am Chem Soc* 1997; **119**: 1529–38.
- 30** Chen CC, Rahil J, Pratt RF *et al*. Structure of a phosphonate-inhibited  $\beta$ -lactamase. An analog of the tetrahedral transition state/intermediate of  $\beta$ -lactam hydrolysis. *J Mol Biol* 1993; **234**: 165–78.
- 31** Dryjanski M, Pratt RF. Inactivation of the *Enterobacter cloacae* P99  $\beta$ -lactamase by a fluorescent phosphonate: direct detection of ligand binding at the second site. *Biochemistry* 1995; **34**: 3569–75.
- 32** Lobkovsky E, Billings EM, Moews PC *et al*. Crystallographic structure of a phosphonate derivative of the *Enterobacter cloacae* P99 cephalosporinase: mechanistic interpretation of a  $\beta$ -lactamase transition-state analog. *Biochemistry* 1994; **33**: 6762–72.
- 33** Maveyraud L, Pratt RF, Samama J-P. Crystal structure of an acylation transition-state analog of the TEM-1  $\beta$ -lactamase. Mechanistic implications for class A  $\beta$ -lactamases. *Biochemistry* 1998; **37**: 2622–8.
- 34** Pratt RF. Inhibition of a class C  $\beta$ -lactamase by a specific phosphonate monoester. *Science* 1989; **246**: 917–9.
- 35** Rahil J, Pratt RF. Mechanism of inhibition of the class C  $\beta$ -lactamase of *Enterobacter cloacae* P99 by phosphonate monoesters. *Biochemistry* 1992; **31**: 5869–78.
- 36** Webster LT Jr. Studies of the acetyl coenzyme A synthetase reaction. V. The requirement for monovalent and divalent cations in partial reactions involving enzyme-bound acetyl adenylate. *J Biol Chem* 1967; **242**: 1232–40.
- 37** Schall OF, Suzuki I, Murray CL *et al*. Characterization of acyl adenyl anhydrides: differences in the hydrolytic rates of fatty acyl-AMP and aminoacyl-AMP derivatives. *J Org Chem* 1998; **63**: 8661–7.
- 38** Jordheim LP, Durantel D, Zoulim F *et al*. Advances in the development of nucleoside and nucleotide analogues for cancer and viral diseases. *Nat Rev Drug Discov* 2013; **12**: 447–64.